

Multi-gap superconductivity in single crystals of $\text{Ba}_{0.65}\text{Na}_{0.35}\text{Fe}_2\text{As}_2$: A calorimetric investigation

A. K. Pramanik,* M. Abdel-Hafez, S. Aswartham, A. U. B. Wolter, S. Wurmehl, V. Kataev, and B. Büchner
Institute for Solid State Research, IFW Dresden, D-01171 Dresden, Germany
 (Dated: November 29, 2018)

We investigate the electronic properties and the superconducting gap characteristics of a single crystal of hole-doped 122 Fe-pnictide $\text{Ba}_{0.65}\text{Na}_{0.35}\text{Fe}_2\text{As}_2$ by means of specific heat measurements. The specific heat exhibits a pronounced anomaly around the superconducting transition temperature $T_c = 29.4$ K, and a small residual part at low temperature. In a magnetic field of 90 kOe, the transition is broadened and T_c is lowered insignificantly by an amount ~ 1.5 K. We estimate a high electronic coefficient in the normal state with a value $57.5 \text{ mJ mol}^{-1} \text{ K}^2$, being consistent with hole-doped 122 compounds. The temperature-dependent superconducting electronic specific heat cannot be described with single-gap BCS theory under weak coupling approach. Instead, our analysis implies a presence of two *s*-wave like gaps with magnitudes $\Delta_1(0)/k_B T_c = 1.06$ and $\Delta_2(0)/k_B T_c = 2.08$ with their respective weights of 48% and 52%. While our results have qualitative similarities with other hole-doped 122 materials, the gap's magnitude and their ratio are quite different.

PACS numbers: 74.70.Xa, 74.25.Bt, 65.40.Ba, 74.20.Rp

I. INTRODUCTION

The recent discovery of superconductivity (SC) in Fe-based pnictides¹ has led to wide research activities in both experimental and theoretical frontiers of solid state physics.^{2,3} This is primarily because Fe-pnictides exhibit a high transition temperature (T_c), a layered structure, and a proximity between magnetism and SC in its phase diagram - a scenario reminiscent of cuprates. However, Fe-pnictides are multiband metals where all five Fe-*3d* orbitals contribute to the electronic structure in the vicinity of the Fermi surface (FS) having a stark contrast with cuprates which are single band Mott-insulators. Detailed band structure calculations, indeed, show that the FS in Fe-pnictides is characterized by two electron-like cylinders around the *M* point, and two hole-like cylinders plus a 3D heavy hole-like pocket around the Γ point, thereafter implying it a possible multiband superconductor.^{4,5}

As for superconductors in general, the central issue remains to understand the superconducting gap symmetry and the mechanism for Cooper pairing, which are still under debate in case of Fe-pnictides. With a weak electron-phonon coupling in this class of materials,⁵⁻⁷ theoretical calculations predict unconventional SC mediated by antiferromagnetic (AFM) spin fluctuations, and an s_{\pm} type superconducting gap symmetry where the order parameter requires a sign change between different sheets of the FS.^{5,8,9} Experimental findings yet exhibit no consensus on the gap symmetry. For instance, nearly isotropic two full gaps with different magnitudes are evidenced in angle resolved photoemission spectroscopy (ARPES) experiments for both electron- and hole-doped 122 Fe-pnictides.¹⁰⁻¹⁴ A similar situation is observed in other studies, like, point contact Andreev reflection spectroscopy (PCARS),¹⁵ and penetration depth measurements.¹⁶⁻¹⁸ On the other hand, possible existence of nodes is revealed in the temperature (T) dependence of penetration depth and nuclear magnetic

resonance (NMR) measurements for both the 122 and 1111 series.^{19,20} It can be mentioned that most of these investigations (except NMR) are surface sensitive, therefore, sample impurity or inhomogeneity at the surface may cause such contradicting results.

In this situation, specific heat (C) rather provides a key source of information regarding the bulk thermodynamic properties, exploring the electronic- and gap-structure in materials. In addition, it probes the system in equilibrium and low energy state. Recent specific heat studies in different families of Fe-pnictides have explored dissimilar gap properties with a single to double gaps and even the presence of nodes, and this variation appears related to the nature as well as the level of doping.²¹⁻²⁸

In this contribution we investigate the electronic properties and superconducting gap characteristics in a hole-doped 122 compound, $\text{Ba}_{0.65}\text{Na}_{0.35}\text{Fe}_2\text{As}_2$ ($T_c = 29.4$ K), by means of specific heat measurements. Although, such investigations have been performed in great details for its K-doped analogues $\text{Ba}_{1-x}\text{K}_x\text{Fe}_2\text{As}_2$, such studies are lacking in the Na-doped 122 family. It is, however, necessary to scrutinize how these properties are sensitive to different dopant species with unlike sizes and chemistry, considering the fact that the gap properties significantly modify with the nature of the doping elements. To be precise, ARPES experiments reveal that for hole-doped $\text{Ba}_{0.6}\text{K}_{0.4}\text{Fe}_2\text{As}_2$, the average gap for the inner hole-like and two electron-like cylinders is similar with a large value ~ 12 meV, while the outer hole cylinder is having a lower value ~ 6 meV.¹⁰ In contrast, for electron-doped $\text{BaFe}_{1.85}\text{Co}_{0.15}\text{As}_2$, the study shows that the inner hole pocket disappears and the average gaps of comparable sizes (6.6 and 5 meV) are observed in the outer hole and two electron cylinders.¹² These observations underline that detailed investigations are necessary in different compositional materials for a generalized understanding of these issues.

Our results show a pronounced specific heat anomaly

at T_c where the jump height is consistent with the T_c value according to recent results on Fe-pnictides. This transition is minimally suppressed in magnetic fields of 90 kOe. Our estimated electronic coefficient in the normal state is high in agreement with other hole-doped 122 compounds. Our analysis further shows that the superconducting electronic specific heat cannot be described with the single-band weak-coupling BCS scheme, rather it implies the presence of two s -wave like gaps with different magnitudes and contributions. These results have qualitative similarities with K-doped materials. However, the quantitative difference in the gap ratio may indicate the different density of states (DOS) in respective bands and the different interband interaction in these materials, hence highlighting the element specific role of the dopant.

II. EXPERIMENTAL DETAILS

Single crystals of $\text{Ba}_{0.65}\text{Na}_{0.35}\text{Fe}_2\text{As}_2$ (BNFA) and BaFe_2As_2 (BFA) used in the present study have been grown using a self-flux method. The details of sample preparation and characterization are described elsewhere.^{29,30} The parent compound, i.e., BaFe_2As_2 has been used to estimate the lattice specific heat contribution. The crystals have been characterized with x-ray diffraction (XRD) which implies the absence of any chemical impurity phase within the experimental accuracy. The mentioned chemical compositions of this material have been determined by energy dispersive analysis of x-ray (EDAX) spectroscopy performed at different places of the sample. For the sample BNFA, the Na variation in the used piece is found within the instrumental error limit. A recent study on polycrystalline $\text{Ba}_{1-x}\text{Na}_x\text{Fe}_2\text{As}_2$ shows an unstable crystallographic phase in Na-rich compositions where the material is susceptible to chemical impurity phases owing to the large mismatch in the size of Ba^{2+} and Na^{1+} ions.³¹ In view of this, our results regarding the crystal homogeneity are remarkable. The BNFA crystal used in this study is about $2.47 \times 1.98 \times 0.13 \text{ mm}^3$. The magnetization (M) data have been collected using a SQUID-VSM magnetometer made by Quantum Design. The heat capacity is measured along the crystallographic c axis with a Physical Property Measurement System (Quantum Design) using a thermal relaxation technique down to 1.8 K and magnetic fields up to 90 kOe.

III. RESULTS AND DISCUSSIONS

In Fig. 1a we present the temperature dependence of the volume susceptibility (χ_{vol}) measured following the zero-field-cooled (ZFC) and field-cooled (FC) protocols for BNFA. χ_{vol} has been deduced from the demagnetization data measured in a field of 20 Oe applied parallel to the c axis. Care has been taken to correct

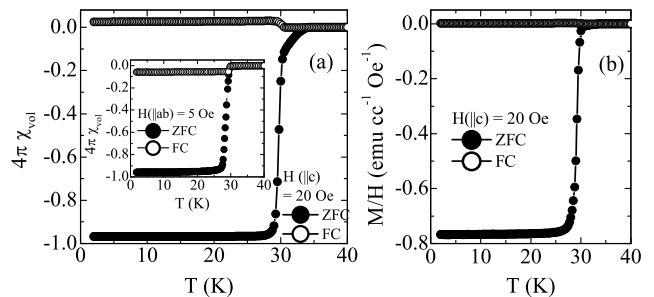


FIG. 1: (a) The volume susceptibility χ_{vol} after demagnetization correction has been plotted as function of temperature. The χ_{vol} has been deduced from the dc magnetization measured with $H||c = 20$ Oe following ZFC and FC protocols for $\text{Ba}_{0.65}\text{Na}_{0.35}\text{Fe}_2\text{As}_2$. The inset shows the similarly deduced χ_{vol} with $H||ab$ plane ($H = 5$ Oe). (b) The same data in main panel of (a) have been plotted without demagnetization correction.

the magnetization data for demagnetization effect where the demagnetization factor has been estimated from an ellipsoidal approximation based on the dimensions of the crystal.³² The material exhibits bulk SC which is evident from the diamagnetic signal in the M_{ZFC} curve at low temperatures. Although, the ZFC and FC magnetization already start to bifurcate around 34 K, our material shows a sharp superconducting transition (width ~ 1.5 K) around 29.7 K determined from the inflection point in dM_{ZFC}/dT . However, similarly deduced χ_{vol} with $H||ab$ plane ($H = 5$ Oe) shows a clear bifurcation between the ZFC and FC magnetization data around 29.5 K, as evident from the inset of Fig. 1a. This difference in onset of bifurcation between our ZFC and FC magnetization data for fields applied along different crystallographic directions will be studied in more detail in the future. Notably, χ_{vol} exhibits an almost full diamagnetic shielding at low temperatures with fields parallel to both c axis and ab plane. These results are in support of the good quality of our single crystal. The fact, that $M_{FC} > 0$ for $H||c$ axis within the superconducting state seems to be an artifact in the data, probably arising from flux trapping during the FC process which is likely for this field geometry due to layered structure in this material. Fig. 1b shows the same data presented in main panel of Fig. 1a without demagnetization correction, demonstrating anomalies are not significantly evident. We would like to mention that the onset of negative magnetization at temperatures higher than the sharp transition in Fig. 1 with $H||c$ axis is not visible in the specific heat data which exhibit a sharp jump around 29.4 K observed in the M_{ZFC} curve (shown below).

The temperature dependence of the specific heat in the form C/T vs T is shown in Fig. 2 for BFA in 0 Oe and for BNFA in 0 and 90 kOe. For our further analysis, the electronic contribution to the specific heat (C_{el}) is required for the material under study (BNFA). Since BNFA is nonmagnetic, the subtraction of the lattice spe-

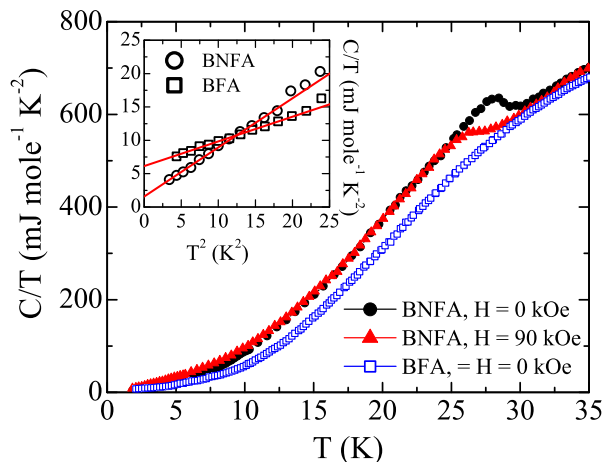


FIG. 2: (Color online) Temperature dependence of the specific heat C/T measured in 0 and 90 kOe for $\text{Ba}_{0.65}\text{Na}_{0.35}\text{Fe}_2\text{As}_2$ and BaFe_2As_2 . The inset shows the plot C/T vs T^2 . The straight lines represent linear fits to $C/T = \gamma + \beta T^2$ (see text).

cific heat (C_{ph}) from the total specific heat (C_{tot}) will simply serve our purpose. Conventionally, C_{ph} is estimated by suppressing the superconducting transition in high magnetic fields. However, the upper critical field (H_{c2}) is significantly high in this class of superconductors. Thus, we have estimated C_{ph} from its parent compound BFA, which is not superconducting throughout the temperature range, as evident from Fig. 2 where C/T does not exhibit any anomalous behavior as function of temperature. On cooling from room temperature, BFA exhibits a long-range magnetic order of AFM-type paired with spin density wave (SDW) formation around 140 K,^{33,34} implying a likely magnetic contribution to its specific heat. In fact, our specific heat data show a sharp peak around this AFM-SDW transition in BFA (not shown). However, a recent neutron scattering measurement has revealed that the energy gap for low-energy spin-wave excitations in the magnetically ordered state is about 9.8 meV ($\equiv 114$ K) for this material.³⁵ Therefore, magnetic contributions to the specific heat will be negligible in the range of our working temperatures (< 35 K), and the specific heat can be assumed to consist of electronic and lattice contributions only.

The compound BNFA, on the other hand, shows an anomaly in C/T around 29.4 K (Fig. 2), which is marked by the superconducting transition. The temperature where this anomaly appears is consistent with the sharp superconducting transition in magnetization measurements (see Fig. 1). The jump in the specific heat is reasonably pronounced with a $\Delta C/T_c$ value around $84 \text{ mJ mol}^{-1} \text{ K}^{-2}$ which is comparable to other hole (potassium) doped 122 compounds with a quantity around $100 \text{ mJ mol}^{-1} \text{ K}^{-2}$.^{22,24,36} It is worth to mention that the obtained $\Delta C/T_c$ for the present material scales well with its T_c in perspective of recent results of Fe-pnictides.³⁷ The

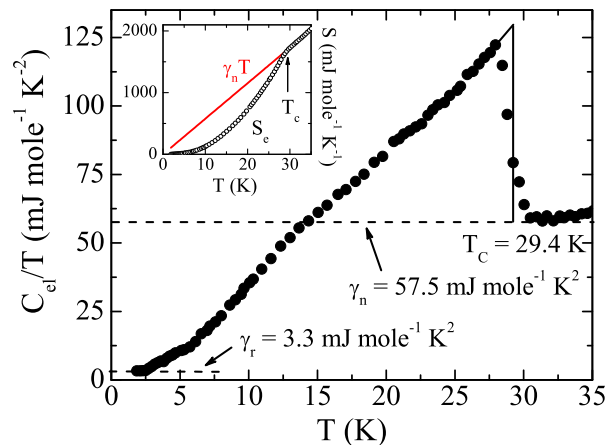


FIG. 3: The electronic specific heat C_{el}/T as function of temperature for the sample $\text{Ba}_{0.65}\text{Na}_{0.35}\text{Fe}_2\text{As}_2$. γ_n and γ_r represent the normal state and residual electronic coefficient of the specific heat. The inset shows the entropy in the normal and superconducting state as a function of temperature.

specific heat measured in a magnetic field of 90 kOe (Fig. 2) shows that the superconducting transition is broadened and insignificantly shifted (~ 1.5 K) in 90 kOe for BNFA, which is expected from its high H_{c2} estimated to be above 100 Tesla.^{36,38}

In the inset of Fig. 2, specific heat data have been plotted in the form C/T vs T^2 for the compounds BFA and BNFA. At low temperature, the data can be linearly fitted to $C/T = \gamma + \beta T^2$, where γ and β are the electronic and lattice coefficients of the specific heat.³⁹ For BFA, we obtain $\gamma = 6.13(8) \text{ mJ mol}^{-1} \text{ K}^{-2}$ and $\beta = 0.369(7) \text{ mJ mol}^{-1} \text{ K}^{-4}$. From the obtained β -value, we calculate the Debye temperature θ_D following the relation $\theta_D = [(12\pi^4 Rn)/(5\beta)]^{1/3}$, where R is the molar gas constant, and n is the number of atoms per formula unit.³⁹ This gives $\theta_D = 297$ K for BFA. The extracted value of γ in our crystal is consistent with other studies on single crystals of BFA ($\sim 6.1 \text{ mJ mol}^{-1} \text{ K}^{-2}$),^{40,41} and close to theoretically predicted values, i.e., $5.68 \text{ mJ mol}^{-1} \text{ K}^{-2}$ (Ref. 42) or $7.22 \text{ mJ mol}^{-1} \text{ K}^{-2}$ (Ref. 43). The fact that the specific heat data C/T versus T^2 for BNFA exhibit a linear behavior at low temperatures without any upturn discards the possibility of Schottky-like contributions in our sample under study.

The phononic contribution C_{ph} to the specific heat of BFA has been determined following the relation $C_{ph}^{BFA} = C_{tot}^{BFA} - C_{el}^{BFA}$, where the C_{el}^{BFA} is $\gamma^{BFA} \cdot T$. We find that the specific heat is dominated by phonons in this region, i.e., around T_c , C_{el} is only about 10% of C_{ph} . Using $C_{el}^{BNFA}/T = C_{tot}^{BNFA}/T - f \cdot C_{ph}^{BFA}/T$, we can calculate C_{el}^{BNFA} . The scaling factor f has been introduced due to slightly different atomic compositions between BNFA and BFA. To determine the value of f , we have used a criterion that normal- and superconducting-state entropy are equal at T_c , i.e., $\int_0^{T_c} (C_{el}/T) dT = \gamma_n T_c$, where γ_n is the normal-state electronic specific heat coefficient. We

TABLE I: The superconducting transition temperature T_c , the jump height of the electronic specific heat $\Delta C_{el}/T_c$, the normal state electronic specific heat coefficient γ_n , and the superconducting gap properties α_i and γ_i/γ_n extracted from specific heat measurements for $\text{Ba}_{0.65}\text{Na}_{0.35}\text{Fe}_2\text{As}_2$ along with other hole- and electron-doped 122 Fe-pnictides. The α_i and γ_i/γ_n represent the zero temperature gap ratio and its weight in the i -th band, respectively.

Compounds	Ref.	T_c (K)	$\Delta C_{el}/T_c$ (mJ mol ⁻¹ K ⁻²)	γ_n (mJ mol ⁻¹ K ⁻²)	$\alpha_i = \Delta_i(0)/k_B T_c, \gamma_i/\gamma_n$
$\text{Ba}_{0.65}\text{Na}_{0.35}\text{Fe}_2\text{As}_2^a$	This work	29.4	72.5	57.5	$\alpha_1=1.06, \gamma_1/\gamma_n=0.48$ $\alpha_2=2.08, \gamma_2/\gamma_n=0.52$
$\text{Ba}_{0.6}\text{K}_{0.4}\text{Fe}_2\text{As}_2^a$	22	36.5	98.1	63.3	$\alpha_1=1.945, \gamma_1/\gamma_n=1$
$\text{Ba}_{0.6}\text{K}_{0.4}\text{Fe}_2\text{As}_2^b$	23	37.3	~ 100	49	$\alpha_1=2.07, \gamma_1/\gamma_n=1$
$\text{Ba}_{0.68}\text{K}_{0.32}\text{Fe}_2\text{As}_2^a$	24	38.5	~ 120	50	$\alpha_1=1.1, \gamma_1/\gamma_n=0.5$ $\alpha_2=3.3, \gamma_2/\gamma_n=0.5$
$\text{KFe}_2\text{As}_2^b$	25	3.5	~ 21	69.1	$\alpha_1=0.3, \gamma_1/\gamma_n=0.55$ $\alpha_2=2.4, \gamma_2/\gamma_n=0.45$
$\text{Ba}(\text{Fe}_{0.925}\text{Co}_{0.075})_2\text{As}_2^a$	26,27	21.4	30	23.8	$\alpha_1=0.95, \gamma_1/\gamma_n=0.33$ $\alpha_2=2.2, \gamma_2/\gamma_n=0.67$
$\text{Ba}(\text{Fe}_{0.92}\text{Co}_{0.08})_2\text{As}_2^a$	28	20	~ 22	18	$\alpha_1=0.957, \gamma_1/\gamma_n=0.38$ $\alpha_2=2.175, \gamma_2/\gamma_n=0.62$

^aSingle crystal

^bPolycrystal

started with $f = 1$ but the entropy conservation criterion is satisfied for $f = 0.95$ (inset of Fig. 3). This practice yields $T_c = 29.4$ K. The resulting C_{el}/T for BNFA is presented in the main panel of Fig. 3. It is obvious from the figure that the superconducting transition at T_c is reasonably sharp, yielding a jump in C_{el}/T at T_c around 72.5 mJ mol⁻¹ K⁻². From our determined $\gamma_n = 57.5$ mJ mol⁻¹ K⁻², we estimate the universal parameter $C_{el}/\gamma_n T_c = 1.26$. This value, however, is lower than the weak-coupling BCS prediction of 1.43.⁴⁵ Following the fact that the superconducting anomaly at T_c is reasonably sharp in BNFA, therefore a distribution in T_c or the presence of an impurity phase is an unlikely explanation for such a reduced value of $C_{el}/\gamma_n T_c$. Instead, we believe that the presence of multiple SC gaps possibly render a low $C_{el}/\gamma_n T_c$ in BNFA, as evidenced in other 122 Fe-pnictides.^{25,26,28} Moreover, the signature of a multi-gap scenario in BNFA is evidenced by a significant hump around 12 K in our C_{el}/T vs T data (Fig. 3), which will be discussed below. Note that C_e/T almost saturates at low temperature, however, it does not extrapolate to zero, yielding a residual electronic specific heat value $\gamma_r = 3.3$ mJ mol⁻¹ K⁻². We mention that the presence of a finite γ_r is common in both electron- and hole-doped 122 crystals,^{22-24,26,27} and that the value of γ_r in our present case is remarkably low, showing the good quality of our single crystal. The origin of γ_r in BNFA is not clear, however, it may arise due to an incomplete transition to the superconducting state or broken pairs in the superconducting condensate.^{26,27,44} Nonetheless, assuming a superconducting volume fraction $(\gamma_n - \gamma_r)/\gamma_n \approx 95\%$, our crystal consists of a high value, which is in fair agreement with our magnetization data (Fig. 1).

The obtained high value of γ_n for BNFA is consistent with other members in the hole-doped 122 series whereas for electron-doped 122 compounds γ_n is much lower (see

Table I). Utilizing our value for γ_n , we can obtain information about the normal state electronic properties, i.e., the DOS at the Fermi energy $N(\epsilon_F)$ of BNFA using the relation:⁴⁶

$$\gamma_n = \gamma_0 (1 + \lambda), \quad (1)$$

$$\gamma_0 = \frac{\pi^2 k_B^2}{3} N(\epsilon_F), \quad (2)$$

where λ is the electron-phonon coupling constant and k_B is the Boltzmann constant. Since in the case of Fe-pnictides λ is not significant, we can set $\gamma_n \equiv \gamma_0$. Therefore, γ_n is mainly contributed by $N(\epsilon_F)$ which implies a higher $N(\epsilon_F)$ in hole-doped compounds than in electron-doped ones. From our γ_n , we calculate $N(\epsilon_F) = 24.37$ states eV⁻¹ f.u.⁻¹. It is worth to mention that the general high values of γ_n or $N(\epsilon_F)$ for hole-doped 122 Fe-pnictides remains controversial with theoretical calculations yielding $\gamma_n = 13.03$ mJ mol⁻¹ K⁻² and $N(\epsilon_F) = 5.526$ states eV⁻¹ f.u.⁻¹ for $\text{Ba}_{0.5}\text{K}_{0.5}\text{Fe}_2\text{As}_2$, where the related values are only around 20% higher than the parent compound.⁴⁷ However, another calculation clarifies that upon including the band parameters from experimental ARPES data as well as mass renormalization effects, the calculated γ_n is close to the experimental values.⁴⁸ Nonetheless, this controversy calls for further rigorous theoretical investigations adopting possible reconciliations within the experimental findings.

After exploring the electronic specific heat and electronic structure, we now examine the superconducting gap properties in BNFA. In many cases, specific heat measurements have already been proved to be an effective tool in understanding the superconducting gap structure

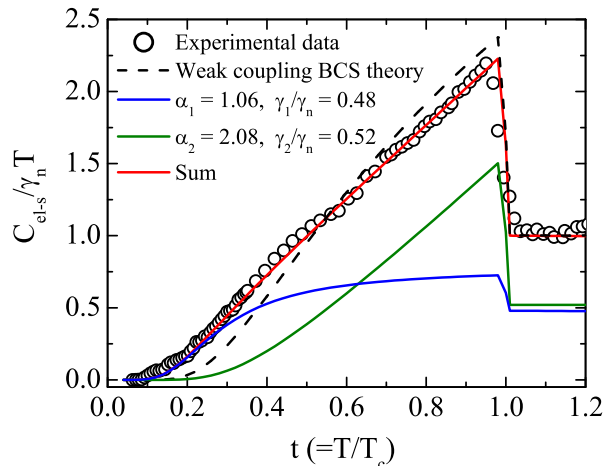


FIG. 4: The normalized superconducting electronic specific heat ($C_{el-s}/\gamma_n T$) of $\text{Ba}_{0.65}\text{Na}_{0.35}\text{Fe}_2\text{As}_2$ as a function of reduced temperature $t = T/T_c$. The dashed line represents the theoretical curve based on single-band weak coupling BCS theory with the s -wave gap $\Delta(0)/k_B T_c = 1.76$ following Eq. 4 and 5. The solid lines represent the curves of the two s -wave gap model (see text).

and its distributions.^{49,50} For our sample, however, C_{el} first needs to be corrected due to a finite γ_r . At low temperature C_{el} is assumed to be contributed by the superconducting (C_{el-s}) as well as the non-superconducting normal (C_n) parts of the specific heat. While the normal electrons will have specific heat contributions linear in temperature ($\gamma_r T$) the superconducting electronic contribution will be scaled by $1 - \gamma_r/\gamma_n$. On this basis, the sum of the individual contributions to C_{el} allows to extract C_{el-s} from the following relation:

$$C_{el-s}/T = \frac{\gamma_n}{\gamma_n - \gamma_r} (C_{el}/T - \gamma_r). \quad (3)$$

In Fig. 4 we present the normalized data $C_{el-s}/\gamma_n T$ as a function of reduced temperature $t (= T/T_c)$ for BNFA. As mentioned earlier, $C_{el-s}/\gamma_n T$ exhibits a broad hump around $t = 0.4$, which implies the presence of multiple SC gaps in this compound. We have analyzed our specific heat data utilizing the α -model which was originally proposed to account for the thermodynamic properties of a strongly coupled single-gap superconductor under semiempirical approach.⁴⁹ This model, however, later had been generalized to explain the specific heat behavior in multi-band, multi-gap superconductors, i.e., MgB_2 .⁵⁰ Following this model, the thermodynamic properties like the entropy (S) and C can be calculated for a system of independent quasiparticles as:^{49,50}

$$\frac{S}{\gamma_n T_c} = -\frac{6}{\pi^2} \frac{\Delta(0)}{k_B T_c} \int_0^\infty [f \ln f + (1-f) \ln(1-f)] dy, \quad (4)$$

$$\frac{C}{\gamma_n T_c} = t \frac{d(S/\gamma_n T_c)}{dt}, \quad (5)$$

where $f = [\exp(\beta E) + 1]^{-1}$ and $\beta = (k_B T)^{-1}$. The energy of the quasiparticles is given by $E = \sqrt{[\epsilon^2 + \Delta^2(t)]}$, where ϵ is the energy of the normal electrons relative to the Fermi surface. In Eq. 4, the integration variable $y = \epsilon/\Delta(0)$, where $\Delta(0)$ is the zero temperature gap magnitude and the scaled gap $\alpha = \Delta(0)/k_B T_c$ is the only adjustable fitting parameter. The temperature dependence of the gap is determined as $\Delta(t) = \Delta(0)\delta(t)$, with $\delta(t)$ being obtained from the table in Ref. 51. In the case of two gaps, the thermodynamic properties are determined as the sum of contributions from the two gaps, i.e., $\alpha_1 (= \Delta_1(0)/k_B T_c)$ and $\alpha_2 (= \Delta_2(0)/k_B T_c)$ with their respective weights γ_1/γ_n and γ_2/γ_n respectively, where $\gamma_1 + \gamma_2 = \gamma_n$.

Using Eqs. 4 and 5, we first calculate the specific heat $C_{el-s}/\gamma_n T$ as a function of t with $\alpha = 1.76$ for the single-band weak coupling BCS theory. As evident from Fig. 4, the calculations disagree significantly with our experimental data, where the former is characterized by a higher jump anomaly at T_c . Moreover, an opposite curvature and different magnitude below and above $t \approx 0.55$ can be observed for the single-gap model compared to the experimental data. We then calculate $C_{el-s}/\gamma_n T$ introducing two gaps and their appropriate weights. Apparently, values $\alpha_1 = 1.06$ [$\Delta_1(0) = 2.68$ meV], $\gamma_1/\gamma_n = 0.48$ and $\alpha_2 = 2.08$ [$\Delta_2(0) = 5.27$ meV], $\gamma_2/\gamma_n = 0.52$, yield the closest matching with our experimental data (see Fig. 4). The Fig. 4 also shows the $C_{el-s}/\gamma_n T$ vs t plot for an individual α and its weights.

For the sake of comparison, we have summarized the values of scaled gaps α_1 and α_2 and their respective weights, T_c , $\Delta C_{el}/T_c$ and γ_n for $\text{Ba}_{0.65}\text{Na}_{0.35}\text{Fe}_2\text{As}_2$ along with other hole- and electron-doped 122 materials in Table I. For BNFA, the larger gap α_2 has a higher value than the weak-coupling BCS gap value (1.76) while the smaller one α_1 has a lower value. Although the gap magnitudes are scattered for different compounds within the Ba-122 family, their relative weights exhibit a consistent trend. Upon electron doping the smaller gap has around (30 - 40)% contribution to the electronic specific heat, whereas for hole doped compounds both the bands contribute almost equally. While our obtained gap structure for $\text{Ba}_{0.65}\text{Na}_{0.35}\text{Fe}_2\text{As}_2$ has qualitative similarity with other hole doped materials, such as $\text{Ba}_{0.68}\text{K}_{0.32}\text{Fe}_2\text{As}_2$, the gap ratio Δ_2/Δ_1 differs significantly (Table I).

In the scenario of an interband pairing model for Fe-pnictides,⁵² the gap ratio is predicted as $\Delta_2/\Delta_1 = \sqrt{N_1/N_2}$, where N_1 and N_2 are the Fermi-level DOS in the respective bands, and Δ_2/Δ_1 is shown to evolve with the effective coupling among the bands. Therefore, one can speculate that the DOS in different bands as well as their coupling modify with K^{1+} and Na^{1+} doping. Indeed, K^{1+} and Na^{1+} have different ionic sizes

and electronic configurations which may contribute differently to these issues. However, Δ_2/Δ_1 ratio implies that N_1/N_2 in $\text{Ba}_{0.68}\text{K}_{0.32}\text{Fe}_2\text{As}_2$ is surprisingly about twice higher than in $\text{Ba}_{0.65}\text{Na}_{0.35}\text{Fe}_2\text{As}_2$, which seems to be an unlikely situation with just this kind of dopant variation (see Table 1). On the other hand, the fact that $\gamma_1 \sim \gamma_2 \sim 0.5\gamma_n$ for both compounds implies that both gaps open up at the FS with almost equal DOS irrespective of the dopant species. These observations probably suggest that the theoretical discussions in Ref. 52 need to include more than two bands. In fact, ARPES results^{10,11} strongly hint towards the inclusion of at least four bands (two hole-like and two electron-like) opening the superconducting gaps in $\text{Ba}_{1-x}\text{K}_x\text{Fe}_2\text{As}_2$. Also, the need for four bands to describe the thermodynamic signatures has been pointed out in theoretical calculation.⁴⁸ At the same time, one can clearly see in Table 1 that within multi-gap analysis the smaller gap α_1 remains almost close to 1 for all materials (except for the extremely hole-doped case KFe_2As_2). However, the larger one α_2 , which appears in the strongly nested inner hole-like and electron-like bands, varies with both the doping element and their concentration, illustrating that the nesting condition is modified with the doping in Fe-pnictides, which is quite intriguing.

It is worth to mention here that the employed α -model follows a simple semiempirical approach where the superconducting gap is assumed to have BCS temperature dependence and the interband coupling is not taken into account. Despite such simplification this model has been extensively used to analyze the experimental thermodynamic data for many kinds of materials. One, however, certainly needs to check other self-consistent models to compare the results. In this scenario, within the framework of Eliashberg approach for MgB_2 Dolgov *et al.*⁵³ has shown that α -model is sufficiently accurate to find the superconducting gap values though the gap's partial contribution lacks in full agreement. Another recently proposed γ -model by Kogan *et al.*⁵⁴ is also an effective approach which takes into account the interband pairing potential and is successfully tested for two band superconductors MgB_2 and V_3Si . Our experimental work calls therefore for a detailed theoretical analysis of our data with these and other appropriate models to fully understand the multigap superconducting nature in

Fe-pnictides. In addition, considering the fact that superconducting gaps estimated by using different experimental techniques like ARPES, PCARS, or muon spin rotation (μSR) exhibit a wide distribution of absolute values,¹⁴ further studies involving specific heat measurements are required on doped 122 Fe-pnictides with different kinds of doping elements as well as doping concentrations to develop a comprehensive understanding and a generalized view on this matter.

IV. CONCLUSIONS

In summary, the electronic properties and superconducting gap structure of hole doped 122 Fe-pnictide $\text{Ba}_{0.65}\text{Na}_{0.35}\text{Fe}_2\text{As}_2$ are studied by measuring specific heat. A reasonably pronounced anomaly has been found around $T_c = 29.4$ K. In applied magnetic fields, the transition becomes broadened, however, there is only a minimal decrease in T_c of about 1.5 K in 90 kOe. Employing an entropy conservation criterion at T_c , we extract $\gamma_n = 57.5$ mJ mole⁻¹ K⁻² which agrees well with other hole doped 122 compounds. It is interesting that the temperature-dependent superconducting electronic specific heat cannot be explained within single-band weak-coupling BCS theory. From our analysis we find that the presence of *s*-wave like two gaps with magnitudes $\Delta_1(0)/k_B T_c = 1.06$ and $\Delta_2(0)/k_B T_c = 2.08$ and respective weights of about $\gamma_1/\gamma_n = 0.48$ and $\gamma_2/\gamma_n = 0.52$ matches well with our experimental data. Though these results are qualitatively similar to K-doped 122 compounds, on a quantitative level their gap magnitudes and their ratios are quite different. This calls for further studies on materials with different doping levels to reach a full understanding of the gap structure and related mechanisms.

V. ACKNOWLEDGMENT

We acknowledge fruitful discussions with V. Zabolotnyy. We thank M. Deutschmann, S. Müller-Litvanyi, R. Müller, J. Werner, and S. Gaß for technical support. This work has been supported by the DFG, Germany through grant no BE 1749/13 and WO 1532/3-1.

* Electronic address: a.k.pramanik@ifw-dresden.de, ashpramanik@gmail.com, 026403 (2008).

¹ Y. Kamihara, T. Watanabe, M. Hirano, and H. Hosono, *J. Am. Chem. Soc.* **130**, 3296 (2008).

² J. Paglione and R. L. Greene, *Nat. Phys.* **6**, 645 (2010).

³ D. C. Johnston, *Advances in Physics* **59**, 803 (2010).

⁴ D. J. Singh and M.-H. Du, *Phys. Rev. Lett.* **100**, 237003 (2008).

⁵ I. I. Mazin, D. J. Singh, M. D. Johannes, and M. H. Du, *Phys. Rev. Lett.* **101**, 057003 (2008).

⁶ L. Boeri, O. V. Dolgov, and A. A. Golubov, *Phys. Rev.*

⁷ L. Boeri, O. V. Dolgov, and A. A. Golubov, *Physica C* **469**, 628 (2009).

⁸ K. Kuroki, S. Onari, R. Arita, H. Usui, Y. Tanaka, H. Kontani, and H. Aoki, *Phys. Rev. Lett.* **101**, 087004 (2008).

⁹ A. V. Chubukov, D. V. Efremov, and I. Eremin, *Phys. Rev. B* **78**, 134512 (2008).

¹⁰ H. Ding *et al.*, *Europhys. Lett.* **83**, 47001 (2008).

¹¹ D. V. Evtushinsky *et al.*, *Phys. Rev. B* **79**, 054517 (2009).

¹² K. Terashima *et al.*, *Proc. Natl. Acad. Sci. USA* **106**, 7330

- (2009).
- ¹³ L. Wray *et al.*, Phys. Rev. B **78**, 184508 (2008).
 - ¹⁴ D. V. Evtushinsky, D. S. Inosov, V. B. Zabolotnyy, M. S. Viazovska, R. Khasanov, A. Amato, H-H. Klauss, H. Luetkens, Ch. Niedermayer, G. L. Sun, V. Hinkov, C T Lin, A. Varykhalov, A. Koitzsch, M. Knupfer, B Büchner, A. A. Kordyuk and S. V. Borisenko, New J. Phys. **11**, 055069 (2009).
 - ¹⁵ P. Samuely, Z. Pribulová, P. Szab, G. Pristáš, S. L. Budko, P. C. Canfield, Physica C **469**, 507 (2009).
 - ¹⁶ R. Khasanov, D.V. Evtushinsky, A. Amato, H.-H. Klauss, H. Luetkens, Ch. Niedermayer, B. Büchner, G. L. Sun, C. T. Lin, J. T. Park, D. S. Inosov, and V. Hinkov, Phys. Rev. Lett. **102**, 187005 (2009).
 - ¹⁷ T. J. Williams, A. A. Aczel, E. Baggio-Saitovitch, S. L. Budko, P. C. Canfield, J. P. Carlo, T. Goko, J. Munevar, N. Ni, Y. J. Uemura, W. Yu, and G. M. Luke, Phys. Rev. B **80**, 094501 (2009).
 - ¹⁸ C. Martin, M. E. Tillman, H. Kim, M. A. Tanatar, S.K. Kim, A. Kreyssig, R. T. Gordon, M. D. Vannette, S. Nandi, V. G. Kogan, S. L. Budko, P. C. Canfield, A. I. Goldman, and R. Prozorov, Phys. Rev. Lett. **102**, 247002 (2009).
 - ¹⁹ R. T. Gordon, C. Martin, H. Kim, N. Ni, M. A. Tanatar, J. Schmalian, I. I. Mazin, S. L. Budko, P. C. Canfield, and R. Prozorov, Phys. Rev. B **79**, 100506(R) (2009).
 - ²⁰ H.-J. Grafe, D. Paar, G. Lang, N. J. Curro, G. Behr, J. Werner, J. Hamann-Borrero, C. Hess, N. Leps, R. Klingeler, and B. Büchner, Phys. Rev. Lett. **101**, 047003 (2008).
 - ²¹ G. Mu, X-Y. Zhu, L. Fang, L. Shan, C. Ren, H-H. Wen, Chin. Phys. Lett. **25**, 2221 (2008).
 - ²² G. Mu, H. Luo, Z. Wang, L. Shan, C. Ren, and H-H. Wen, Phys. Rev. B **79**, 174501 (2009).
 - ²³ Ch. Kant, J. Deisenhofer, A. Günther, F. Schrettle, and A. Loidl, M. Rotter and D. Johrendt, Phys. Rev. B **81**, 014529 (2010).
 - ²⁴ P. Popovich, A. V. Boris, O. V. Dolgov, A. A. Golubov, D. L. Sun, C. T. Lin, R. K. Kremer, and B. Keimer, Phys. Rev. Lett. **105**, 027003 (2010).
 - ²⁵ H. Fukazawa *et al.*, J. Phys. Soc. Jpn. **78**, 038712 (2009).
 - ²⁶ F. Hardy, T. Wolf, R. A. Fisher, R. Eder, P. Schweiss, P. Adelman, H. v. Löhneysen, and C. Meingast, Phys. Rev. B **81**, 060501(R) (2010).
 - ²⁷ F. Hardy, P. Burger, T. Wolf, R. A. Fisher, P. Schweiss, P. Adelman, R. Heid, R. Fromknecht, R. Eder, D. Ernst, H. v. Löhneysen, and C. Meingast, Europhys. Lett. **91**, 47008 (2010).
 - ²⁸ K. Gofryk, A. S. Sefat, E. D. Bauer, M. A. McGuire, B. C. Sales, D. Mandrus, J. D. Thompson and F. Ronning, New J. Phys. **12**, 023006 (2010).
 - ²⁹ S. Aswartham, C.Nacke, G. Friemel, N. Leps, S. Wurmehl, N. Wizent, C. Hess, R. Klingeler, G. Behr, S. Singh, and B. Büchner, J. Crystal Growth **314**, 341 (2011).
 - ³⁰ S. Aswartham *et al.*, (unpublished).
 - ³¹ R. Cortes-Gil, D. R. Parker, M. J. Pitcher, J. Hadermann, and S. J. Clarke, Chem. Mater. **22**, 4304 (2010). [DOI: 10.1021/cm100956k].
 - ³² J. A. Osborn, Phys. Rev. **67**, 351 (1945).
 - ³³ M. Rotter, M. Tegel, D. Johrendt, I. Schellenberg, W. Hermes, and R. Pöttgen, Phys. Rev. B **78**, 020503(R) (2008).
 - ³⁴ Q. Huang, Y. Qiu, W. Bao, M. A. Green, J. W. Lynn, Y. C. Gasparovic, T. Wu, G. Wu, and X. H. Chen, Phys Rev. Lett. **101**, 257003 (2008).
 - ³⁵ K. Matan, R. Morinaga, K. Iida, and T. J. Sato, Phys. Rev. B, **79**, 054526 (2009).
 - ³⁶ U. Welp, R. Xie, A. E. Koshelev, W. K. Kwok, H. Q. Luo, Z. S. Wang, G. Mu, and H. H. Wen, Phys. Rev. B **79**, 094505 (2009).
 - ³⁷ S. L. Bud'ko, N. Ni, P. C. Canfield, Phys. Rev. B **79**, 220516(R) (2009).
 - ³⁸ Z-S. Wang, H-Q. Luo, C. Ren, and H-H. Wen, Phys. Rev. B **78**, 140501(R) (2008).
 - ³⁹ E. S. R. Gopal *Specific Heats at Low Temperatures* (Plenum Press, New York, 1966).
 - ⁴⁰ J. K. Dong, L. Ding, H. Wang, X. F. Wang, T. Wu, G. Wu, X. H. Chen, and S. Y. Li, New J. Phys. **10**, 123031, (2008).
 - ⁴¹ A. S. Sefat, M. A. McGuire, R. Jin, B. C. Sales, D. Mandrus, F. Ronning, E. D. Bauer, and Y. Mozharivskiy, Phys. Rev. B **79**, 094508 (2009).
 - ⁴² F. Ma, Z-Y. Lu, and T. Xiang, arXiv:0806.3526.
 - ⁴³ D. J. Singh, Phys. Rev. B **78**, 094511 (2008).
 - ⁴⁴ R. A. Fisher, N. E. Phillips, A. Schilling, B. Buffeteau, R. Calemczuk, T. E. Hargreaves, C. Marcenat, K. W. Dennis, R. W. McCallum, and A. S. O'Connor, Phys. Rev. B **61**, 1473 (2000).
 - ⁴⁵ C. P. Poole Jr., H. A. Farach, R. J. Creswick, and R. Prozorov *Superconductivity* 2nd edition, (Academic Press, Amsterdam, 2007).
 - ⁴⁶ C. Kittel *Solid State Physics*, 8th edition (John Wiley and Sons, New York, 2005).
 - ⁴⁷ I. R. Shein and A. L. Ivanovskii, JETP Lett. **88**, 115 (2008).
 - ⁴⁸ L. Benfatto, E. Cappelluti, and C. Castellani, Phys. Rev. B **80**, 214522 (2009).
 - ⁴⁹ H. Padamsee, J. E. Neighbor, A. C. Shiffman, J. Low Temp. Phys. **12**, 387 (1973).
 - ⁵⁰ F. Bouquet, Y. Wang, R. A. Fisher, D. G. Hinks, J. D. Jorgensen, A. Junod, and N. E. Phillips, Europhys. Lett. **56**, 856 (2001).
 - ⁵¹ B. Mühlischlegel, Z. Phys. **155**, 313 (1959).
 - ⁵² O. V. Dolgov, I. I. Mazin, D. Parker, and A. A. Golubov, Phys. Rev. B **79**, 060502(R) (2009).
 - ⁵³ O. V. Dolgov, R. K. Kremer, J. Kortus, A. A. Golubov, and S. V. Shulga, Phys. Rev. B **72**, 024504 (2005).
 - ⁵⁴ V. G. Kogan, C. Martin, and R. Prozorov, Phys. Rev. B **80**, 014507 (2009).